Molecular Cloning, *E. coli* Expression and Characterization of Thermostable Alanine Aminotransferase from *Pyrococcus abyssi*

Muhammad Shahid Nadeem*, Jalaluddin Azam Khan and Firoz Anwar

Department of Biochemistry, Faculty of Science, King Abdulaziz University, Jeddah 21589, Saudi Arabia

ABSTRACT

Catalysing the reversible interconversion of L-alanine and alpha-ketoglutarate to pyruvate and L-glutamate in the presence of pyridoxal 5 phosphate, alanine aminotransferase (ALT) is an enzyme which operates at the cross roads of amino acid and carbohydrate metabolism. The enzyme has been reported from a wide range of organisms including animals, plants, fungi and microbes. The enzyme has a clinical applications in the diagnosis of many diseases. In the present study we have produced a recombinant of ALT from *Pyrococcus abyssi* in BL21 (DE3) strain of *E. coli*. The recombinant enzyme was purified by anion exchange chromatography, it displayed a 45kDa band on SDS-PAGE, with 58.1% final recovery, 15.3 fold purification and 139 U/mg specific activity. Maximum enzyme activity was found at pH 8 and above 90C, its K_M and Vmax values were found 25µM L-alanine and 149 U/min/mg respectively. In silico studies have shown that the enzyme was found in a monomer structure. Molecular docking studies with potential molecules involved in the reaction catalysed have been conducted and binding energy values were calculated for each molecule including L-alanine, pyridoxal 5 phosphate, pyruvate, alpha ketoglutarate and L-glutamate. Present study provides the first report of ALT from *Pyrococcus abyssi* and suggests active site residues of enzyme from archaeal origin.

INTRODUCTION

Alanine aminotransferase (ALT), (EC 2.6.1.2) is the enzyme responsible to catalyse reversible conversion of L-alanine and alpha-ketoglutarate to L-glutamate and pyruvate in the presence of pyridoxal phosphate which acts as a prosthetic group. ALT catalysed reaction provides a link between the amino acid and carbohydrate metabolism by producing pyruvate (an intermediate of carbohydrate metabolism from L-alanine. There are two isoforms of ALT found in the human body, ALT1 or cytosolic form and ALT2 or mitochondrial form, both are coded by different genes. ALT2 is exclusively produced in the heart and skeletal muscles (Mendes-Mourao *et al.*, 1975; Pan *et al.*, 2003; Sato *et al.*, 2004; Shan *et al.*, 2009). ALT is ubiquitous in nature and studied from a wide range of organisms including *Alternaria conidia*, humans, algae such as *Chlamydomonas reinhardtii*, higher plants, and silk worm (Varley *et al.*, 2002; Good *et al.*, 2007; Liu *et al.*, 2008; Good and Beatty, 2011; Inagaki *et al.*, 2012; Lecler *et al.*, 2012; De Linares *et al.*, 2022). There are several clinical and industrial applications of ALT, as for example the human plasma levels of ALT have been used as a biomarker for liver damage or liver diseases (Kim *et al.*, 2008). The enzyme has also been used for the diagnosis of some cancers and muscular dystrophy (Wagner *et al.*, 2021; Muyas *et al.*, 2022). The elevated levels of ALT in blood plasma has also been linked with diabetes, hyperlipidaemia, obesity and cardiovascular diseases (Yun *et al.*, 2009; Bril *et al.*, 2020; Kathak *et al.*, 2022; Saleh *et al.*, 2022). ALT also has applications in the urea producing and pharmaceutical industries (Schreiber *et al.*, 2002; Zia *et al.*, 2021). Increasing demands of ALT and other important enzymes require the recombinant production by heterologous gene expression in a suitable system, *E. coli* based microbial gene expression system provides an economic, timely and simple system for the production of recombinant enzymes (Backlund *et al.*, 2008). The microbial system has a capacity to produce bulk quantities of target enzymes and proteins (Jonet *et al.*, 2012; Jia and Jeon, 2016; Zhou *et al.*, 2018). In the recent times, *in silico* studies have been used for the prediction of 3D

---

protein structure, active site amino acids, binding affinities of substrates and potential inhibitors to the enzyme active site, and ultimately the selection of better enzyme, substrate and inhibitors (Kamble *et al.*, 2019; Comaki *et al.*, 2020). In the present study, we aimed to produce the recombinant ALT from *Pyrococcus abyssi* GE5 strain. The target species is an archaeon that grows at 90 °C under high pressure conditions (Erauso *et al.*, 1993; Cohen *et al.*, 2003). Recombinant of enzyme was produced in *E. coli*, purified by chromatographic techniques, evaluated by kinetics and in silico analysis.

MATERIALS AND METHODS

Materials

All reagents, kits, chemicals, PCR kit, dNTPs, DNA ligation and restriction enzymes, plasmid vectors for cloning, DNA/protein electrophoresis, plasmid isolation, restriction and analysis kits, chromatography columns and reagents were purchased from Thermo Fisher and Sigma-Aldrich. Genomic DNA of archaeon was obtained from DSMZ Germany. All reagents and molecules were of molecular biology grade.

Gene synthesis, sub-cloning, expression, and purification

ALT gene from *Pyrococcus abyssi* GE5 consists of 1197bp open reading frame (ORF). In the ORF, there is a restriction site for *Nde*I (catatg), 147 bp at 5' end, downstream to the start codon (ATG) and a restriction site for *Nco*I (ccatgg) at 188 bp upstream to the stop codon. We found it difficult to subclone the complete open reading frame in pET 21a(+) vector. Hence, the gene was

synthesized commercially from Macrogen (South Korea), it was made available in pUC57 vector (2710 bp) which has ampicillin resistance site (Fig. 1).

The gene harbouring plasmid was used for the transformation of DH-10 cells by using Thermo Scientific. InsTAclone PCR Cloning Kit. #K1214, the successful transformants were grown in LB broth containing 100μg/ml ampicillin to isolate plasmids. Plasmid were isolated using GeneJET Plasmid Miniprep Kit Catalogue number: K0502 (Thermo Fisher-Waltham, Massachusetts, United States). Procedure and instructions given by the manufacturer were followed. The plasmids were confirmed by restriction analysis with *Nde*I and *Bam*HI to generate sticky ends of gene. Same pair of restriction enzymes was used for the restriction of pET21a (+) plasmid vector. ALT gene was ligated into pET21a (+) expression vector using T4 ligase (EL0011- Thermo Fisher - Waltham, Massachusetts, United States), under the conditions provided by the supplier. The recombinant plasmid pET21-alt[+] was confirmed by restriction analysis using *Nde*I and *Bam*HI. The confirmed recombinant cells of BL21 (DE3) strain of *E. coli* were subjected to induction of gene expression. In short, the cells were grown in LB-broth supplemented with 100μg/ml ampicillin, in the log phase of bacterial growth when the OD 600nm of bacterial culture was from 0.5 to 0.6, the expression of *ALT* gene was induced by the addition of 0.5mM IPTG (Isopropyl β-D-1-thiogalactopyranoside), final concentration in the medium. Induced *E. coli* culture was grown for 3.5 h at 37°C and stored at 4°C. The cells were harvested by centrifugation at 7000 rpm for 10 min at 4°C. The cells were sonicated at a medium power for
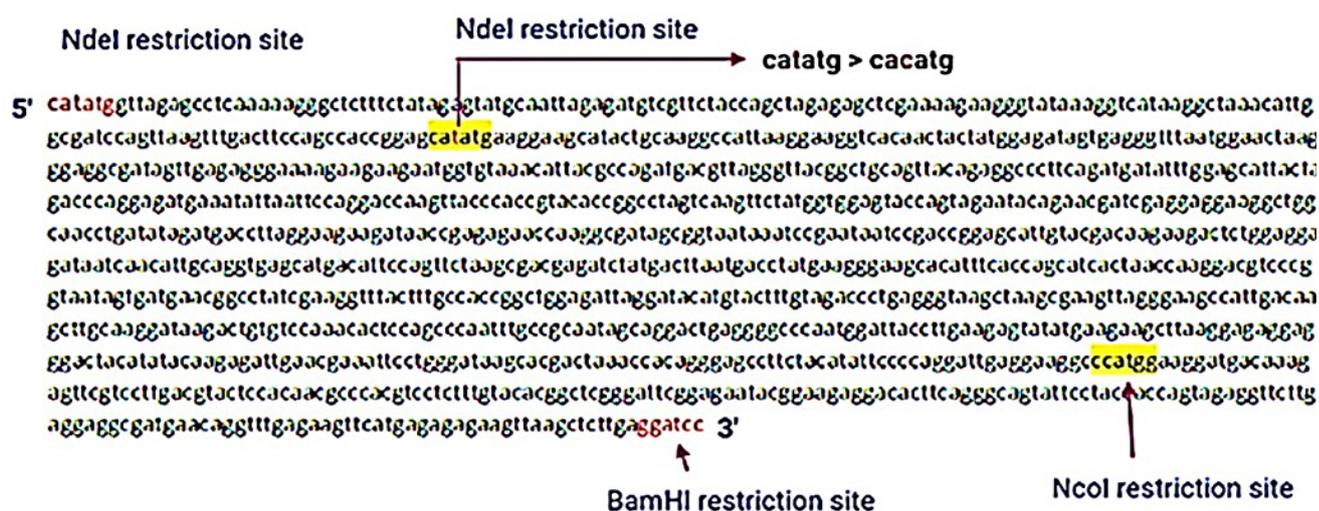
Fig. 1. Sequence of *P. abyssi* gene coding for ALT with restriction sites for *Nde*I, *Nco*I inside the open reading frame (ORF) and restriction site of *Bam*HI.

10 min by repeating 1 min exposure to incubation in the ice-box, alternatively. The cellular residue was removed by centrifugation at 12000 rpm/10 min at 4°C, clear supernatant was retained and subjected to dialysis in 20mM phosphate buffer pH 7.5 adjusted at 4°C (buffer A). The chromatography column (2.5 x 36 cm) was prepared by adding 30 mL of pre-soaked DEAE-Sephadex and equilibrated with buffer A. Dialyzed sample was clarified by centrifugation at 15000 rpm/10min at 4°C and clear supernatant was loaded onto the column at a flow rate of 2.5 mL/min, unbound proteins were washed by using buffer A, enzyme was eluted with an increasing gradient (0 to 0.5M) of sodium chloride (NaCl), fractions of 2 mL were collected, and stored at 4°C.

Characterization of recombinant ALT

All reagents and chemicals used for the enzyme assay were prepared in 20 mM phosphate buffer pH 7.5 (buffer A). The reagents included 1.2M L-alanine, 0.5M α-ketoglutarate, 5 to 7mg/mL of NADH disodium salt, lactate dehydrogenase 300 to 400 international units, and suitable dilution of purified enzyme. Before the measurement of enzyme activity, 100mg PLP was mixed well to 1mL of purified enzyme dilution. A UV/Vis spectrophotometer UV-1900i (Shimadzu Kyoto, Kyoto, Japan) was adjusted at 25°C and 340 nm. A neat clean 2mL capacity glass cuvette was carefully added with 1 mL of L-alanine solution, 150 µL alpha-ketoglutarate, 100 µL NADH solution (freshly prepared), 100 µL of LDH and incubated for 5 min. At the end 10 µL of enzyme was added and mixed well by pipetting. Increase in the reading at 340 nm was noted for 3 min. Total protein content was determined by Bradford *et al.* (1956) by using a standard curve prepared by using bovine serum albumin. The enzyme activity was calculated by the following formula:

$$Enzyme\ activity\left(\frac{U}{mg}\right) = \frac{Reaction\ volume\ (mL)\ x\ Change\ in\ OD340nm\ X\ Enzyme\ dilution\ factor}{6.22\ x\ Enzyme\ volume\ (mL)\ x\ total\ protein\ content\ (mg)}$$

Enzyme activity was determined in the presence of buffer solutions adjusted at different pH values (4, 5, 6, 7, 8, 9, 10), and adjusting the temperature of reaction mixture at variable temperatures (from 30°C to 90°C); optimum pH and temperature for the enzyme activity were calculated. Enzyme stability was determined after 10 min of incubation of enzyme at different temperatures (60°C, 70°C, 80°C, 90°C, 100°C) prior to enzyme assay keeping the other conditions constant. The enzyme activity was also calculated by regular increase in the substrate concentration under optimum pH and temperature conditions to determine the K_M and V_{max} values of enzyme by Lineweaver-Burk plot. Enzyme activity was also measured under optimum conditions in the presence of 100µM of copper (Cu), cadmium (Cd), iron (Fe), manganese (Mn), lead (Pb), chromium (Cr), magnesium (Mg), calcium (Ca), to determine the effect of these ions on the enzyme activity.

Protein modeling and validation

Protein structure of alanine aminotransferase from *Pyrococcus abyssi* was built using I-TASSER server (Yang *et al.*, 2015), which develops 3D models from the structure templates identified by LOMETS from the PDB library. The templates of the highest significance in the threading alignments is selected by I-TASSER. Subsequently, the quality of the predicted model was examined by RAMPAGE, a protein structure validation server (Lovell *et al.*, 2003; Wang *et al.*, 2016), which reveals the results in terms of phi, psi and C-beta deviations by generating a Ramachandran plot for the protein built.

Structural alignment

After the structure assembly simulation, TM-align structural alignment program (Zhang and Skolnick, 2005; Madhusudhan *et al.*, 2009), was employed to match the first I-TASSER model to all the structures in PDB library. Due to the structural similarity, these protein often have similar functions to the target. High TM-Score represents closest structural similarity.

Docking analysis

The 3D model was then prepared for docking analysis, by eliminating hetero atoms including water molecules and performing energy minimization by PyMol (Yuan *et al.*, 2017; Faure *et al.*, 2019), and ModRefiner (Xu and Zhang, 2011; Dhorajiwala *et al.*, 2019), respectively. The PDB structures of selected ligands, i.e., alanine, alpha-ketoglutarate, pyruvate, glutamate and pyridoxal-5-phosphate were downloaded from ChemSpider chemical database. All selected ligands were docked against the ALT-PA protein model using Hex docking server (Macindoe *et al.*, 2010; Ritchie and Venkatraman, 2010). The ΔG (binding free energy) of each docked protein-ligand complex was recorded to analyze the binding nature of the complexes.

RESULTS

Production, purification and properties of recombinant ALT

Under the T7 promoter system, a recombinant of ALT from *P. abyssi* was successfully generated in *E. coli* cells. It was purified up to 15.3 folds by anion exchange chromatography with more than 58% final recovery. The purified enzyme has shown a specific activity of 138 U/mg of protein, it displayed a 45 kDa protein band on SDS-PAGE (Table I, Fig. 2).

Table I. Purification of ALT produced as recombinant in *E. coli*. A unit of enzyme is defined as the amount of enzyme that can convert one micromole of L-alanine and alpha-ketoglutarate into products in one minute under our experimental conditions.

| Purification step	Specific activity (U/mg)	Total units	Percentage recovery	Fold purification
Crude cellular extract	9.0	5400	100	1
Dialysate	9.8	4800	88.88	1.08
DEAE- column chromatography	138	3140	58.14	15.3
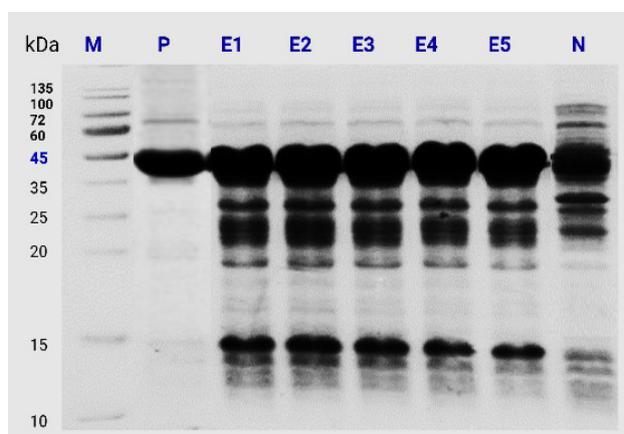
Fig. 2. SDS-PAGE of purified enzymes, M, protein marker; P, purified enzyme; E1, E2, E3, E4, and E5- extract of experimental cells with gene expression; N, negative control.
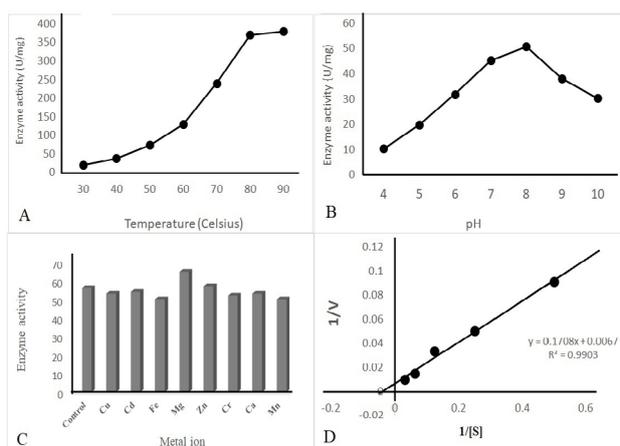

Fig. 3. Kinetic properties of purified recombinant ALT indicating maximum activity at pH 8, above 90◦C and in the presence of Mg^{2+} ions. K_M and V_{max} values were calculated as 25µM of L-alanine and 149.25 U/mg, respectively.

Purified enzyme has shown activity at a wide range of temperatures and pH with an optimum activity at above 90◦C and pH 8. More than 50% enzyme activity was retained when incubated at 100◦C for 10 minutes indicating a high temperature stability. The measurement of activity in the presence of different metal ions has shown a significant increase in the enzyme activity in the presence of Mg^{2+} ions. Purified ALT investigated in the present study has shown a K_M value of 25 µM L-alanine and V_{max} 149.25U/mg/min (Fig. 3).

Protein modeling and validation

I-TASSER generated the ALT-PA protein model has been generated (visualization by PyMOL Molecular Graphics System, Version 1.2r3pre.), by using 1XI9 as a homologous template, which determines the crystal structure of ALT from *Pyrococcus furiosus*. The quality assessment by Ramachandran plot reveals that the template-based structure of ALT from *P. abyssi* was quite stable, with >99% of residues in the favored and allowed regions (Fig. 4).
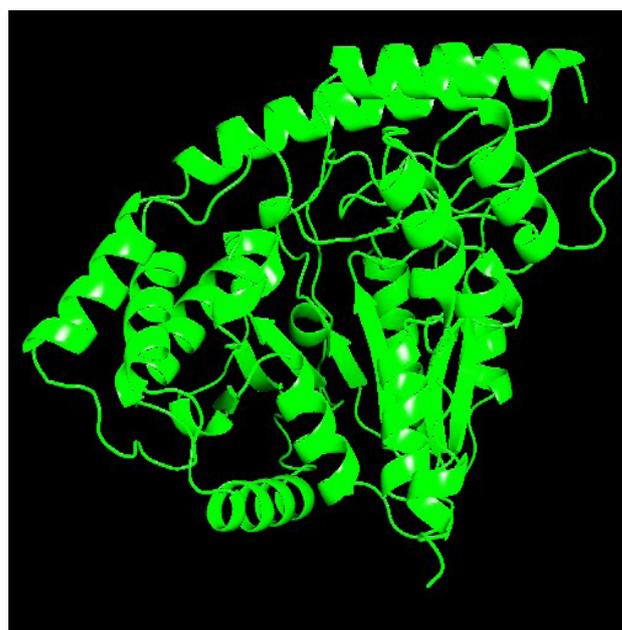
Fig. 4. 3D model of ALT-PA represented as cartoon (Green) (Visualized by PyMol).

The structural alignment results by TM-align shows 1xi9A to be ranked number 1 as the template crystal model (1XI9) contained identical residues in its protein sequence which are structurally 99% identical to that of query with lowest RMSD values when compared to other top PDB hits.

Docking and comparative analysis

Docking results summarized in the Table II revealed that ALT-pyridoxal-5-phosphate complex (Fig. 5A) obtained the lowest free energy corresponding to highest binding affinity, followed by ALT-glutamate (Fig. 5C), ALT-alpha-ketoglutarate (Fig. 5E), ALT-L alanine (Fig. 5H) and ALT-pyruvate (Fig. 5I) docked complexes.
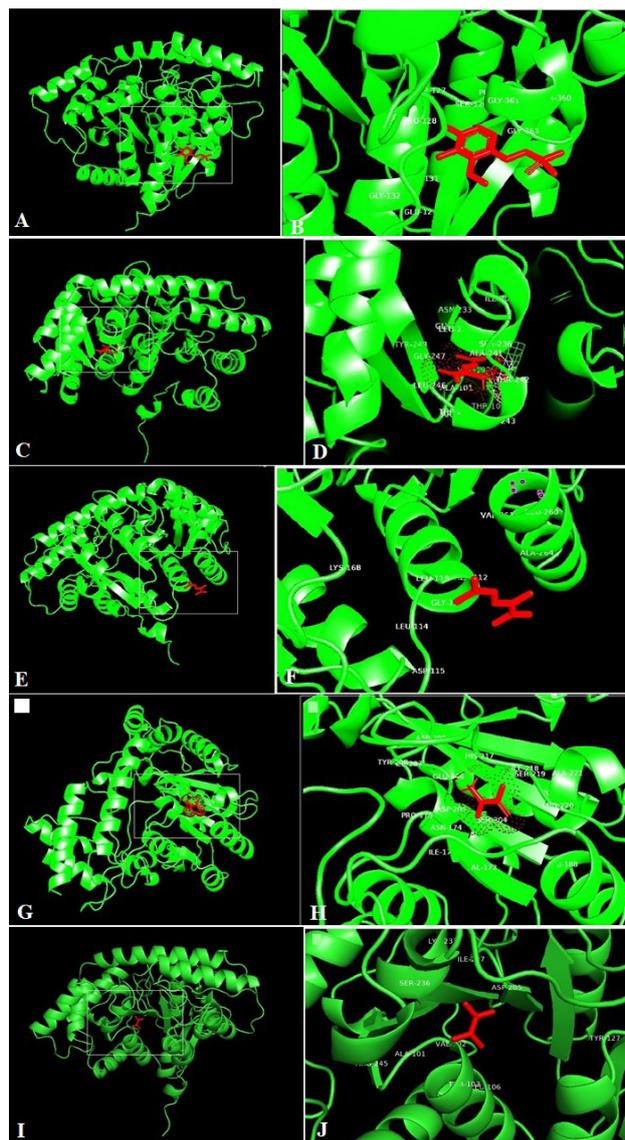

Fig. 5. Docked complexes showing alanine aminotransferase in green pyridoxal-5-phosphate (A), glutamate (C), α ketoglutarate (E), alanine (G) and pyruvate (I) as red sticks. Zoomed view of ALT-pyridoxal-5-phosphate docked complex (B), ALT-glutamate (D), ALT- α-ketoglutarate (F) ALT-alanine (H) ALT-pyruvate docked complex (J) with interactive residues under 5Å (Visualization by PyMol).

Table II. TM-align results showing the comparison of top identical structures from PDB database with the modeled 3D structure of ALT from *P. abyssi*.

Rank[a]	PDB Hit	TM-score[b]	RMSD[c]	IDEN[d]	Cov[e]
1	1xi9A	0.986	0.32	0.924	0.987
2	4cvqA	0.950	1.66	0.383	0.990
3	1bw0B	0.948	1.68	0.294	0.990
4	4ix8A	0.941	1.69	0.261	0.982
5	3tcmA	0.941	1.81	0.281	0.993
6	6f77A	0.939	1.24	0.331	0.965
7	6f35A	0.937	1.33	0.317	0.967
8	5wmhA	0.934	1.25	0.340	0.960
9	1gd9A	0.923	1.48	0.396	0.955
10	1j32A	0.920	1.67	0.308	10

[a] Ranking of proteins is based on TM-score of the structural alignment between the query structure and known structures in the PDB library. [b] Template Modeling Score (TM-score) measure the structural similarity between two structures TM-score >0.5 indicates a model of correct topology and a TM-score<0.17 means a random similarity range 0 to 1). [c] Heavy atoms Root-Mean-Square Deviation (RMSD) with respect to the experimental structure. [d] IDEN is the percentage sequence identity in the structurally aligned region (range 0 to 1. [e] Cov represents the coverage of global structural alignment and is equal to the number of structurally aligned residues divided by length of the query protein cluster. (range 0 to 1).

DISCUSSION

ALT is an enzyme of amino acid metabolism that also links the amino acid metabolism and carbohydrate metabolism. The enzyme is widely distributed in natural world such as in plant, animals, fungi and bacteria (Ward *et al*., 2000; Hosono *et al*., 2003; Duan *et al*., 2009; Good and Beatty, 2011). ALT has a great clinical importance, it has been extensively used as a biomarker for the diagnosis of liver diseases, liver injuries, it serves as a biosensor, diagnosis of dengue fever, detection of hepatitis B and C (Li *et al*., 2006; Senior, 2012; EASL, 2014; Gao *et al*., 2017; Wang *et al*., 2018; Ayaz and Furrukh, 2020). The present study was aimed at the recombinant production, purification, kinetics and *in silico* properties of enzyme from *Pyrococcus abyssi* which is a hyperthermophilic archaeon, unexplored for most of its enzyme, including ALT. The ALT coding gene has been investigated from a wide range of species including man to higher animals, and plants to bacteria. These genes coding for ALT in different species have shown different nucleotide sequences and properties of their protein products. All this information based on gene sequences and subsequent protein characteristics contribute to the pool of literature on ALT

Table III. Binding free energies of the docked complexes with ALT-PA and selected ligands.

Protein	Ligand	ΔG(kJ/mol)	Binding residues
ALT-PA	Pyridoxal-5-phosphate	-221.58	12, 126, 127, 128, 131, 132, 360, 361, 362, 363
	Glutamate	-170.84	101, 102, 103, 207, 233, 234, 235, 236, 241, 242, 243, 244, 245, 246, 247, 248
	Alpha-ketoglutarate	-162.48	111, 112, 113, 114, 115, 168, 260, 261, 264
	Alanine	-128.84	86, 172, 173, 174, 175, 188, 204, 205, 206, 207, 208, 209, 217, 218, 219, 220, 221
	Pyruvate	-112.58	38, 101, 102, 103, 106, 127, 205, 207, 236, 237, 245

Note: ΔG represents binding free energies of docked complex of respective protein and ligand.

(Shrawat *et al.*, 2008; Parthasarathy *et al.*, 2019). In the present study, a gene coding for alanine aminotransferase from *Pyrococcus abyssi* (Fig. 1). has been cloned in *E. coli* and the properties of its corresponding recombinant protein have been investigated. The commercially synthesized gene was restricted out from pUC57 plasmid vector and introduced into pET 21a (+) expression vector, the later was used for the transformation of BL21 (DE3) strain of *E. coli.* The confirmed recombinant *E. coli* cells were grown to their early log phase with 0.5 to 0.6 optical density at 600nm and gene expression was induced in the presence of 0.5mM final concentration of IPTG. Similar IPTG concentrations have been successfully used for the production of recombinant heterologous proteins (Assadi-Porter *et al.*, 2008; Dvorak *et al.*, 2015). The expressed enzyme was purified by chromatography; it has shown a molecular weight of 44 kDa on SDS-PAGE (Fig. 2). The enzyme with molecular weight of 54 kDa, 45 kDa, 94 kDa, and 50 kDa has been reported from different animal and plant species (Orzechowski *et al.*, 1999; Liepman and Olsen, 2001; Yang *et al.*, 2002; Kendziorek *et al.*, 2012). The enzyme being reported in the present report has shown optimum activity at pH 8, and above 90°C. It was stable at a wide pH range and temperature up to 100°C, Mg^{2+} ions increased the enzyme activity, the values of K_M and V_{max} of enzyme was 25µM L-alanine and 149.25U/mg, respectively (Fig. 3). Enzyme isolated from a similar species, *Pyrococcus furiosus*, has shown optimum activity at pH 6.5 to 7.8 and 95°C. However, the K_M value for this enzyme was 2.8mM L-alanine was high as compared to the enzyme being reported from *P. abyssi* (Ward *et al.*, 2000). K_M values of 5.0 mM has also been reported from bacterial species (Oikawa, 2006). There is no information available about the effect of metal ions on the activity of ALT. 3D structure based on *in silico* studies has shown that the enzyme exists as a monomer (Fig. 4). A monomer structure of enzyme has been reported in literature (Duff *et al.*, 2012). Molecular docking studies with potential substrate molecules have shown the active site residues and binding affinities of enzyme with these molecules (Fig.

5). The docking structures were verified by using different alignment tools (Table II). Docking studies have shown binding energy of ΔG -221.58 kJ/mol with pyridoxal-5-phosphate, ΔG -170.84 kJ/mol with L-glutamate, ΔG -162.48 kJ/mol with alpha-ketoglutarate, ΔG -128.84 kJ/mol with L-alanine, ΔG -112.58 kJ/mol with pyruvate (Table III). ALT active site residues of enzyme from *E. coli* reported in a study include Tyr15, Tyr37 and Tyr152, Arg18 and Tyr129 (Pena-Soler *et al.*, 2014). However, there are only a few studies available about the active site analysis of bacterial and archaeal ALT, the information provided by the in silico analysis will provide a baseline for the future research in these lines.

CONCLUSIONS

The present study provides insights into the clinically important enzyme from an unexplored species. The enzyme investigated in the study was stable at high temperatures with maximum activity above 90°C indicating its potential in the industries. In silico studies have demonstrated binding affinities of different potential substrate molecules to the enzyme active site. The information acquired from the computer based studies require further confirmation by crystal structure analysis in the presence of substrate and PLP.

REFERENCES

Assadi-Porter, F.M., Patry, S., and Markley, J.L., 2008. Efficient and rapid protein expression and purification of small high disulfide containing sweet protein brazzein in *E. coli*. *Protein Expres. Purif.*, **58**: 263–268. https://doi.org/10.1016/j.pep.2007.11.009

Ayaz, F., and Furrukh, M. 2020. Assessment of severity of dengue fever by deranged alanine aminotransferase levels. *Cureus*, **12**: e10539. https://doi.org/10.7759/cureus.10539

Bäcklund, E., Reeks, D., Markland, K., Weir, N., Bowering, L., and Larsson, G., 2008. Fedbatch design for periplasmic product retention in *Escherichia coli*. *J. Biotechnol.*, **135**: 358–365. https://doi.org/10.1016/j.jbiotec.2008.05.002

Bradford, E.B., Vanderhoff, J.W. and Alfrey Jr, T., 1956. The use of monodisperse latexes in an electron microscope investigation of the mechanism of emulsion polymerization. *J. Coll. Sci.*, **11:** 135-149. https://doi.org/10.1016/0095-8522(56)90033-2

Bril, F., McPhaul, M.J., Caulfield, M.P., Clark, V.C., Soldevilla-Pico, C., Firpi-Morell, R.J., Lai, J., Shiffman, D., Rowland, C.M., and Cusi, K., 2020. Performance of plasma biomarkers and diagnostic panels for nonalcoholic steatohepatitis and advanced fibrosis in patients with type 2 diabetes. *Diabetes care*, **43**: 290–297. https://doi.org/10.2337/dc19-1071

Cohen, G.N., Barbe, V., Flament, D., Galperin, M., Heilig, R., Lecompte, O., Poch, O., Prieur, D., Quérellou, J., Ripp, R., Thierry, J.C., Van der Oost, J., Weissenbach, J., Zivanovic, Y., and Forterre, P., 2003. An integrated analysis of the genome of the hyperthermophilic archaeon *Pyrococcus abyssi*. *Mol. Microbiol.*, **47**: 1495–1512. https://doi.org/10.1046/j.1365-2958.2003.03381.x

Comakli, V., Adem, S., Oztekin, A., and Demirdag, R. 2020. Screening inhibitory effects of selected flavonoids on human recombinant aldose reductase enzyme: *In vitro* and in silico study. *Arch. Physiol. Biochem.,* pp. 1–7. https://doi.org/10.1080/13813455.2020.1771377

De Linares, C., Navarro, D., Puigdemunt, R., and Belmonte, J., 2022. Airborne Alt a 1 dynamic and its relationship with the airborne dynamics of alternaria conidia and pleosporales spores. *J. Fungi*, **8**: 125. https://doi.org/10.3390/jof8020125

Dhorajiwala, T.M., Halder, S.T. and Samant, L., 2019. Comparative in silico molecular docking analysis of l-threonine-3-dehydrogenase, a protein target against African trypanosomiasis using selected phytochemicals. *J. appl. Biotechnol. Rep.*, **6**: 101-108. https://doi.org/10.29252/JABR.06.03.04

Duan, Y., Guo, J., Wang, S., Yu, X., Huang, L. and Kang, Z., 2009. Cloning and expression analysis of alanine aminotransferase gene TaAlaAT1 in wheat infected with stripe rust fungus. *Acta Phytopathol. Sin.*, **39**: 139-146.

Duff, S.M., Rydel, T.J., McClerren, A.L., Zhang, W., Li, J.Y., Sturman, E.J., Halls, C., Chen, S., Zeng, J., Peng, J., Kretzler, C.N., and Evdokimov, A., 2012. The enzymology of alanine aminotransferase (AlaAT) isoforms from Hordeum vulgare and other organisms, and the HvAlaAT crystal structure. *Arch. Biochem. Biophys.*, **528**: 90–101. https://doi.org/10.1016/j.abb.2012.06.006

Dvorak, P., Chrast, L., Nikel, P. I., Fedr, R., Soucek, K., Sedlackova, M., Chaloupkova, R., de Lorenzo, V., Prokop, Z., and Damborsky, J., 2015. Exacerbation of substrate toxicity by IPTG in *Escherichia coli* BL21(DE3) carrying a synthetic metabolic pathway. *Microb. Cell Fact.,* **14**: 201. https://doi.org/10.1186/s12934-015-0393-3

Erauso, G., Reysenbach, A.L., Godfroy, A., Meunier, J.R., Crump, B., Partensky, F., Baross, J.A., Marteinsson, V., Barbier, G., Pace, N.R. and Prieur, D., 1993. *Pyrococcus abyssi* sp. nov., a new hyperthermophilic archaeon isolated from a deep-sea hydrothermal vent. *Arch. Microbiol.,* **160**: 338-349. https://doi.org/10.1007/BF00252219

European Association for Study of Liver. 2014. EASL clinical practice guidelines: Management of hepatitis C virus infection. *J. Hepatol.*, **60**: 392–420. https://doi.org/10.1016/j.jhep.2013.11.003

Faure, G., Joseph, A.P., Craveur, P., Narwani, T.J., Srinivasan, N., Gelly, J.C., Rebehmed, J., de Brevern, A.G. 2019. iPBAvizu: A PyMOL plugin for an efficient 3D protein structure superimposition approach. *Source Code Biol. Med.*, **14**: 5. https://doi.org/10.1186/s13029-019-0075-3

Gao, S., Li, X.Y., Fan, Y.C., Sun, F.K., Han, L.Y., Li, F., Ji, X.F., and Wang, K., 2017. A noninvasive model to predict liver histology in HBeAg-positive chronic hepatitis B with alanine aminotransferase ≤2upper limit of normal. *J. Gastroenterol. Hepatol.*, **32**: 215–220. https://doi.org/10.1111/jgh.13452

Good, A.G., and Beatty, P.H., 2011. Biotechnological approaches to improving nitrogen use efficiency in plants: Alanine aminotransferase as a case study. In:

The molecular and physiological basis of nutrient use efficiency in crops. pp. 165-191. https://doi.org/10.1002/9780470960707.ch9

Good, A.G., Johnson, S.J., De Pauw, M., Carroll, R.T., Savidov, N., Vidmar, J., Lu, Z., Taylor, G. Stroeher, V., 2007. Engineering nitrogen use efficiency with alanine aminotransferase. *Botany*, **85**: 252-262. https://doi.org/10.1139/B07-019

Hosono, A., Mizuguchi, H., Hayashi, H., Goto, M., Miyahara, I., Hirotsu, K., Kagamiyama, H., 2003. Glutamine:phenylpyruvate aminotransferase from an extremely thermophilic bacterium, Thermus thermophilus HB8. *J. Biochem.*, **134**: 843–851. https://doi.org/10.1093/jb/mvg210

Inagaki, Y., Matsumoto, Y., Kataoka, K., Matsuhashi, N., and Sekimizu, K., 2012. Evaluation of drug-induced tissue injury by measuring alanine aminotransferase (ALT) activity in silkworm hemolymph. *BMC Pharmacol. Toxicol.*, **13:** 13. https://doi.org/10.1186/2050-6511-13-13

Jia, B., and Jeon, C.O., 2016. High-throughput recombinant protein expression in *Escherichia coli*: Current status and future perspectives. *Open Biol.*, **6**: 160196. https://doi.org/10.1098/rsob.160196

Jonet, M.A., Mahadi, N.M., Murad, A.M., Rabu, A., Bakar, F.D., Rahim, R.A., Low, K.O., and Illias, R.M., 2012. Optimization of a heterologous signal peptide by site-directed mutagenesis for improved secretion of recombinant proteins in *Escherichia coli*. *J. Mol. Microbiol. Biotech.*, **22**: 48–58. https://doi.org/10.1159/000336524

Kamble, A., Srinivasan, S., and Singh, H., 2019. In-silico bioprospecting: Finding better enzymes. *Mol. Biotechnol.*, **61**: 53–59. https://doi.org/10.1007/s12033-018-0132-1

Kathak, R.R., Sumon, A.H., Molla, N.H., Hasan, M., Miah, R., Tuba, H.R., Habib, A., and Ali, N., 2022. The association between elevated lipid profile and liver enzymes: A study on Bangladeshi adults. *Scient. Rep.,* **12**: 1711. https://doi.org/10.1038/s41598-022-05766-y

Kendziorek, M., Paszkowski, A., and Zagdańska, B., 2012. Biochemical characterization and kinetic properties of alanine aminotransferase homologues partially purified from wheat (*Triticum aestivum* L.). *Phytochemistry*, **82**: 7–14. https://doi.org/10.1016/j.phytochem.2012.07.008

Kim, W.R., Flamm, S.L., Di Bisceglie, A.M., and Bodenheimer, H.C., 2008. Serum activity of alanine aminotransferase (ALT) as an indicator of health and disease. *Hepatology* (Baltimore, Md.), **47**: 1363–1370. https://doi.org/10.1002/hep.22109

Lecler, R., Vigeolas, H., Emonds-Alt, B., Cardol, P., and Remacle, C., 2012. Characterization of an internal type-II NADH dehydrogenase from *Chlamydomonas reinhardtii* mitochondria. *Curr. Genet.*, **58**: 205–216. https://doi.org/10.1007/s00294-012-0378-2

Li, H., Guo, Z., Wang, H., Cui, D., and Cai, X., 2006. An amperometric bienzyme biosensor for rapid measurement of alanine aminotransferase in whole blood. *Sens. Actuators B Chem.*, **119**: 419-424. https://doi.org/10.1016/j.snb.2005.12.041

Liepman, A.H., and Olsen, L.J., 2001. Peroxisomal alanine: Glyoxylate aminotransferase (AGT1) is a photorespiratory enzyme with multiple substrates in *Arabidopsis thaliana. Pl. J. Cell mol. Biol.*, **25**: 487–498. https://doi.org/10.1046/j.1365-313x.2001.00961.x

Liu, L., Zhong, S., Yang, R., Hu, H., Yu, D., Zhu, D., Hua, Z., Shuldiner, A.R., Goldstein, R., Reagan, W.J., and Gong, D.W., 2008. Expression, purification, and initial characterization of human alanine aminotransferase (ALT) isoenzyme 1 and 2 in High-five insect cells. *Protein Expr. Purif.*, **60**: 225–231. https://doi.org/10.1016/j.pep.2008.04.006

Lovell, S.C., Davis, I.W., Arendall, W.B., de Bakker, P.I., Word, J.M., Prisant, M.G., Richardson, J.S., and Richardson, D.C., 2003. Structure validation by Calpha geometry: Phi, psi and Cbeta deviation. *Proteins*, **50**: 437–450. https://doi.org/10.1002/prot.10286

Macindoe, G., Mavridis, L., Venkatraman, V., Devignes, M.D. and Ritchie, D.W., 2010. HexServer: An FFT-based protein docking server powered by graphics processors. *Nucl. Acids Res.*, **38**: 445-449. https://doi.org/10.1093/nar/gkq311

Madhusudhan, M.S., Webb, B.M., Marti-Renom, M.A., Eswar, N., and Sali, A., 2009. Alignment of multiple protein structures based on sequence and structure features. *Protein Eng. Des. Sel.*, **22**: 569–574. https://doi.org/10.1093/protein/gzp040

Mendes-Mourāo, J., Halestrap, A.P., Crisp, D.M., and Pogson, C.I., 1975. The involvement of mitochondrial pyruvate transport in the pathways of gluconeogenesis from serine and alanine in isolated rat and mouse liver cells. *FEBS Lett.*, **53**: 29–32. https://doi.org/10.1016/0014-5793(75)80674-0

Muyas, F., Rodriguez, M.J.G., Cortes-Ciriano, I., and Flores, I., 2022. The ALT pathway generates telomere fusions that can be detected in the blood of cancer patients. *BioRxiv*, https://doi.org/10.1101/2022.01.25.477771

Oikawa, T., 2006. Alanine, aspartate, and asparagine metabolism in microorganisms. In: *Amino acid biosynthesis~ pathways, regulation and metabolic engineering.* Springer, Berlin, Heidelberg. pp. 273-288. https://doi.org/10.1007/7171_2006_062

Orzechowski, S., Socha-Hanc, J., and Paszkowski, A., 1999. Alanine aminotransferase and glycine aminotransferase from maize (*Zea mays* L.) leaves. *Acta Biochim. Pol*., **46**: 447–457. https://doi.org/10.18388/abp.1999_4176

Pan, Y., Chen, H., Siu, F., and Kilberg, M.S., 2003. Amino acid deprivation and endoplasmic reticulum stress induce expression of multiple activating transcription factor-3 mRNA species that, when overexpressed in HepG2 cells, modulate transcription by the human asparagine synthetase promoter. *J. biol. Chem*., **278**: 38402–38412. https://doi.org/10.1074/jbc.M304574200

Parthasarathy, A., Adams, L.E., Savka, F.C., and Hudson, A.O., 2019. The *Arabidopsis thaliana* gene annotated by the locus tag At3g08860 encodes alanine aminotransferase. *Pl. Direct*, **3**: e00171. https://doi.org/10.1002/pld3.171

Peña-Soler, E., Fernandez, F.J., López-Estepa, M., Garces, F., Richardson, A.J., Quintana, J.F., Rudd, K.E., Coll, M., and Vega, M.C., 2014. Structural analysis and mutant growth properties reveal distinctive enzymatic and cellular roles for the three major L-alanine transaminases of *Escherichia coli*. *PLoS One*, **9**: e102139. https://doi.org/10.1371/journal.pone.0102139

Ritchie, D.W., and Venkatraman, V., 2010. Ultra-fast FFT protein docking on graphics processors. *Bioinformatics* (Oxford, England), **26**: 2398–2405. https://doi.org/10.1093/bioinformatics/btq444

Saleh, M., Kim, J.Y., March, C., Gebara, N., and Arslanian, S., 2022. Youth prediabetes and type 2 diabetes: Risk factors and prevalence of dysglycaemia. *Pediatr. Obes.*, **17**: e12841. https://doi.org/10.1111/ijpo.12841

Sato, H., Nomura, S., Maebara, K., Sato, K., Tamba, M., and Bannai, S. 2004. Transcriptional control of cystine/ glutamate transporter gene by amino acid deprivation. *Biochem. biophys. Res. Commun*., **325**: 109–116. https://doi.org/10.1016/j.bbrc.2004.10.009

Schreiber, W., Alt, T., Edelmann, M., and Malzkorn-Edling, S., 2002. Augmented reality for industrial applications-a new approach to increase productivity. *Proceedings of the 6th international scientific conference on work with display units.*

pp. 380-381.

Senior, J.R., 2012. Alanine aminotransferase: A clinical and regulatory tool for detecting liver injury-past, present, and future. *Clin. Pharmacol. Ther*., **92**: 332–339. https://doi.org/10.1038/clpt.2012.108

Shan, J., Ord, D., Ord, T., and Kilberg, M.S., 2009. Elevated ATF4 expression, in the absence of other signals, is sufficient for transcriptional induction via CCAAT enhancer-binding protein-activating transcription factor response elements. *J. biol. Chem*., **284**: 21241–21248. https://doi.org/10.1074/jbc.M109.011338

Shrawat, A.K., Carroll, R.T., DePauw, M., Taylor, G.J., and Good, A.G., 2008. Genetic engineering of improved nitrogen use efficiency in rice by the tissue-specific expression of alanine aminotransferase. *Pl. Biotechnol. J*., **6**: 722–732. https://doi.org/10.1111/j.1467-7652.2008.00351.x

Varley, H., Pickett, H.A., Foxon, J.L., Reddel, R.R., and Royle, N.J., 2002. Molecular characterization of inter-telomere and intra-telomere mutations in human ALT cells. *Nat. Genet*., **30**: 301–305. https://doi.org/10.1038/ng834

Wagner, K.R., Guglieri, M., Ramaiah, S.K., Charnas, L., Marraffino, S., Binks, M., Vaidya, V.S., Palmer, J., Goldstein, R., and Muntoni, F., 2021. Safety and disease monitoring biomarkers in Duchenne muscular dystrophy: results from a Phase II trial. *Biomarkers Med*., **15:** 1389–1396. https://doi.org/10.2217/bmm-2021-0222

Wang, L., Chen, M., Xu, M., Li, J., Feng, P., He, R., Zhu, Y., Li, H., Lin, J., and Zhang, C., 2018. Ratio of creatine kinase to alanine aminotransferase as a biomarker of acute liver injury in dystrophinopathy. *Dis. Markers*, pp. 6484610. https://doi.org/10.1155/2018/6484610

Wang, W., Xia, M., Chen, J., Deng, F., Yuan, R., Zhang, X., and Shen, F., 2016. Data set for phylogenetic tree and Rampage Ramachandran plot analysis of SODs in *Gossypium raimondii* and *G. arboreum*. *Data Brief.*, **9**: 345–348. https://doi.org/10.1016/j.dib.2016.05.025

Ward, D.E., Kengen, S.W., van Der Oost, J., and de Vos, W.M., 2000. Purification and characterization of the alanine aminotransferase from the hyperthermophilic *Archaeon pyrococcus furiosus* and its role in alanine production. *J. Bact*., **182**: 2559–2566. https://doi.org/10.1128/JB.182.9.2559-2566.2000

Xu, D., and Zhang, Y., 2011. Improving the physical realism and structural accuracy of protein models by a two step atomic level energy

minimization. *Biophys. J.*, **101**: 2525–2534. https://doi.org/10.1016/j.bpj.2011.10.024

Yang, J., Yan, R., Roy, A., Xu, D., Poisson, J., and Zhang, Y., 2015. The I-TASSER Suite: Protein structure and function prediction. *Nat. Methods*, **12**: 7–8. https://doi.org/10.1038/nmeth.3213

Yang, R.Z., Blaileanu, G., Hansen, B.C., Shuldiner, A.R., and Gong, D.W., 2002. cDNA cloning, genomic structure, chromosomal mapping, and functional expression of a novel human alanine aminotransferase. *Genomics,* **79**: 445–450. https://doi.org/10.1006/geno.2002.6722

Yuan, S., Chan, H.S. and Hu, Z., 2017. Using PyMOL as a platform for computational drug design. *Wires Comp. mol. Sci.*, **7**: e1298. https://doi.org/10.1002/wcms.1298

Yun, K.E., Shin, C.Y., Yoon, Y.S., and Park, H.S., 2009. Elevated alanine aminotransferase levels predict mortality from cardiovascular disease and diabetes in Koreans. *Atherosclerosis*, **205**: 533–537. https://doi.org/10.1016/j.atherosclerosis.2008.12.012

Zhang, Y., and Skolnick, J., 2005. TM-align: A protein structure alignment algorithm based on the TM-score. *Nucl. Acids Res*., **33**: 2302–2309. https://doi.org/10.1093/nar/gki524

Zhou, Y., Lu, Z., Wang, X., Selvaraj, J.N., and Zhang, G., 2018. Genetic engineering modification and fermentation optimization for extracellular production of recombinant proteins using *Escherichia coli*. *Appl. Microbiol. Biotechnol*., **102**: 1545–1556. https://doi.org/10.1007/s00253-017-8700-z

Zia, S., Khan, M.R., Shabbir, M.A., and Aadil, R.M., 2021. An update on functional, nutraceutical and industrial applications of watermelon by-products: A comprehensive review. *Trends Fd. Sci. Tech*., **114**: 275-291. https://doi.org/10.1016/j.tifs.2021.05.039